ELSEVIER

Journal of Chromatography A, 915 (2001) 177–183

JOURNAL OF CHROMATOGRAPHY A

www.elsevier.com/locate/chroma

Artificial neural network modeling of Kováts retention indices for noncyclic and monocyclic terpenes

M. Jalali-Heravi*, M.H. Fatemi

Sharif University of Technology, Department of Chemistry, P.O. Box 11365-9516, Tehran, Iran

Received 8 August 2000; received in revised form 13 December 2000; accepted 15 December 2000

Abstract

A quantitative structure–property relationship study based on multiple linear regression (MLR) and artificial neural network (ANN) techniques was carried out to investigate the retention behavior of some terpenes on the polar stationary phase (Carbowax 20 M). A collection of 53 noncyclic and monocyclic terpenes was chosen as data set that was randomly divided into two groups, a training set and a prediction set consist of 41 and 12 molecules, respectively. A total of six descriptors appearing in the MLR model consist of one electronic, two geometric, two topological and one physicochemical descriptors. Except for the geometric parameters the remaining descriptors have a pronounced effect on the retention behavior of the terpenes. A 6-5-1 ANN was generated by using the six descriptors appearing in the MLR model as inputs. The mean of relative errors between the ANN calculated and the experimental values of the Kováts retention indexs for the prediction set was 1.88%. This is in aggreement with the relative error obtained by experiment.

Keywords: Neural networks, artificial; Retention indices; Regression models; Molecular descriptors; Terpenes

1. Introduction

Terpenes are natural products that exist in many family of plants. Currently, many researchers are interested in the chemistry of terpenes. The separation and identification of terpenes in plant essential oils and other natural and synthetic sources rely heavily on gas chromatography (GC). In some cases GC may be the sole means of identification based on direct comparison of retention times with standards or precise knowledge of the Kováts retention indices (*I* values). Even when combined GC–mass spectroscopy (MS) is used for the analysis, assignments often cannot be made on the basis of MS data only. This is due to the fact that many terpenes have essentially similar structures, and after ionization, fragmentation and rearrangement in the ion source produce similar patterns [1]. Hence, some knowledge of retention characteristics is required to complement mass spectral data.

A Kováts retention index reports the retention behavior of a compound relative to a standard set of hydrocarbons, utilizing a logarithmic scale. The retention index of compound A, I_A, is defined as:

$$I_A = 100N + 100 \cdot \frac{\log t'_{R(A)} - \log t'_{R(N)}}{\log t'_{R(N+1)} - \log t'_{R(N)}}$$

where $t'_{R(A)}$ is the adjusted retention time of compound A and $t'_{R(N+1)}$ and $t'_{R(N)}$ are the adjusted

*Corresponding author. Tel.: +98-21-600-5718; fax: +98-21-601-2983.

E-mail address: jalali@sina.sharif.ac.ir (M. Jalali-Heravi).

0021-9673/01/$ – see front matter
PII: S0021-9673(00)01274-7

retention times of *n*-alkanes of carbon number $n+1$ and *n*, that are respectively larger and smaller than the adjusted retention time of the unknown [2]. Retention is a phenomenon that is primarily dependent on the interactions between the solute and the stationary phase molecules. The forces associated with these interactions can be related to the geometric and topological structures and electronic environments of the molecule. Quantitative structure–property relationships (QSPRs) have been demonstrated to be a powerful tool for the investigation of the chromatographic parameters. QSPRs have been used to obtain simple models to explain and predict the chromatographic behavior of various classes of compounds [3]. Mekenyan et al. have derived a linear quantitative retention–structure model in GC for 41 alkylbenzenes [4]. Dimov and Osman have used QSPRs to relate the chromatographic retention of 38 isoalkanes to their molecular structural features [5]. Welsh et al. have studied the chromatographic data for 31 unsubstituted 3–6 ring polycyclic aromatic hydrocarbons using QSPR methods [6]. Recently, Katritzky et al. have used QSPR techniques for correlation and prediction of GC retention indexes of methyl-branched hydrocarbons produced by insects [7]. Some other works in this area are listed in Refs. [8–15].

Artificial neural networks (ANNs) have been applied to a wide variety of chemical problems such as simulation of mass spectra [16], prediction of carbon-13 NMR chemical shift [17], modeling of ion interaction chromatography [18,19], response surface modeling in HPLC optimization [20] and quantitative structure–activity relationship (QSAR) studies [21–23]. Also the flame ionization detector and thermal conductivity detector response factors for a diverse set of organic molecules were predicted using ANN models developed in our laboratory [24,25].

In the present study an ANN was employed to generate a QSPR model between the molecular based structural parameters (descriptors) and observed retention indexes of some noncyclic and monocyclic terpenes on the polar stationary phase (Carbowax 20 M).

Then the generated ANN was evaluated and applied for the prediction of *I* values of some terpenes. As far as we are aware, this is the first QSPR study using ANNs for the prediction of Kováts retention indices of some terpenes.

2. Experimental

2.1. Data set

The data set of the Kováts retention indices was taken from the values reported by Davies [26]. A collection of 53 noncyclic and monocyclic terpenes was chosen (Table 1). Temperature has quite marked effects on the GC retention indices [3]. Therefore, the observed *I* values that are taken from Ref. [26] are obtained under similar conditions and at 150°C. The *I* values of all compounds included in the data set were obtained on a capillary column with the polar Carbowax 20 M stationary phase. Their Kováts *I* values are in the range 1422–1919 for tetrahydrolinalyl acetate and myrcene-8-ol, respectively. The data set was randomly divided into two groups, a training set and a prediction set containing 41 and 12 compounds, respectively. The training and the prediction sets were used for the model generation and evaluation of the model, respectively.

2.2. Descriptor generation

Retention in GC is the result of competitive solubility of the solute between the mobile and the stationary phases. The molecular structure and chemical properties of the solute determine the type and the extent of the interaction of the solute with these phases. The differences between these properties govern the retention behavior through the column. Due to the diversity of the molecules studied in this work, 35 different descriptors are chosen and listed in Table 2. These parameters encode different aspects of the molecular structure, and consist of eight electronic (1–8), nine geometric (9–17), 17 topological (18–34) and one physicochemical (35) descriptors. Geometric descriptors were calculated using optimized Cartesian coordinate and van der Waals radius of each atom in the molecule [27,28]. Electronic descriptors were calculated using the MOPAC program (Version 6) [29]. Topological descriptors were calculated using two-dimensional representation of the molecules. Some

Table 1
The data set and corresponding observed and ANN predicted values of the retention indexes

Number	Name	I_{obs}	I_{ANN}	E_{rel}%
Training set				
1	Citronellyl formate	1638	1627	−0.67
2	1,2-Dihydrolinalool	1537	1521	−1.04
3	Geranyl formate	1717	1702	−0.87
4	Terpinene-4-yl acetate	1640	1627	−0.79
5	Myrcene-8-ol	1919	1896	−1.20
6	Neoisocarvonmenthyl acetate	1672	1664	−0.48
7	Neryl butyrate	1868	1825	−2.30
8	Isopulegyl acetate	1608	1643	2.17
9	Linalyl butyrate	1698	1676	−1.30
10	Carveyl acetate	1795	1810	0.84
11	Citronellyl isobutyrate	1739	1739	0.00
12	Neryl formate	1700	1718	1.06
13	Geranyl isobutyrate	1821	1821	0.00
14	6,10-Dihydromyrcenol	1473	1501	1.90
15	Isomenthyl acetate	1599	1655	3.50
16	Linalyl acetate	1569	1606	2.36
17	Dihydrocarvyl acetate	1700	1722	1.29
18	Myrcenol	1631	1678	2.88
19	Neryl acetate	1735	1767	1.85
20	Carvomenthyl acetate	1641	1670	1.76
21	Dihydronerol	1725	1780	3.18
22	Linalool	1555	1565	0.64
23	Neoisomenthyl acetate	1623	1651	1.72
24	*cis*-Ocimenol	1660	1708	2.90
25	Tetrahydrolinalyl acetate	1422	1457	2.46
26	Citronellol	1765	1767	0.11
27	Citronellyl acetate	1671	1672	0.05
28	*cis*-β-Terpinyl acetate	1622	1682	3.69
29	Tetrahydrogeranyl acetate	1582	1618	2.27
30	Perillyl acetate	1791	1789	−0.12
31	6,7-Dihydrolinalool	1449	1513	4.41
32	Lavandulol	1707	1687	−1.17
33	Neryl propionate	1794	1856	3.45
34	Nerol	1808	1838	1.66
35	Citronellyl butyrate	1811	1856	2.48
36	Geranyl butyrate	1904	1939	1.84
37	Tetrahydrogeraniol	1675	1723	2.86
38	Tetrahydromyrcenol	1449	1458	0.63
39	Terpinyl acetate	1722	1668	−3.13
40	Linalyl propionate	1624	1629	0.30
41	Tetrahydrolinalool	1431	1459	1.96
Prediction set				
42	*trans*-Carveyl acetate	1759	1749	−0.57
43	α-Citronellol	1760	1789	1.65
44	Citronellyl propionate	1738	1774	2.07
45	Geraniol	1842	1788	−2.93
46	Geranyl propionate	1834	1840	0.33
47	Lavandunyl acetate	1609	1553	−3.48
48	Linalyl isobutyrate	1622	1588	−2.10
49	Menthyl acetate	1600	1652	3.25
50	Neomenthyl acetate	1569	1599	1.91
51	Tetrahydrolavandulol	1600	1562	−2.38
52	Nerylisobutyrate	1790	1791	0.05
53	*trans*-Ocimenol	1685	1717	1.90

Table 2
List of descriptors employed in this work

Number	Name
1	Electron density on the most positive atom
2	Electron density on the most negative atom
3	Highest occupied molecular orbital
4	Lowest unoccupied molecular orbital
5	Total dipole moment
6	Highest molecular moment of inertia
7	Lowest molecular moment of inertia
8	Molecular polarizability
9	Shape factor
10	Molecular volume
11	Molecular surface area
12	Molecular shadow area in the z–y plane
13	Molecular shadow area in the x–y plane
14	Molecular shadow area in the x–z plane
15	Molecular standard shadow area in the z–y plane
16	Molecular standard shadow area in the x–y plane
17	Molecular standard shadow area in the x–z plane
18	Zero order connectivity index
19	Path one connectivity index
20	Path two connectivity index
21	Path three connectivity index
22	Path four connectivity index
23	Cluster three connectivity index
24	Cluster four connectivity index
25	Second order kappa index
26	Number of atoms in each molecule
27	Molecular mass
28	Balaban index
29	Number of double bonds in a molecule
30	Number of oxygen atoms in a molecule
31	Number of carbon atoms in a molecule
32	Number of ester groups in a molecule
33	Number of carbonyl groups in a molecule
34	Winer number
35	Molecular density

of the descriptors generated for each compound encoded similar information about the molecule of interest. Therefore, it was desirable to test each descriptor and eliminate those which show high correlation ($R>0.95$) with each other. A total of 13 out of 35 descriptors showed high correlation and was removed from the consideration. Subsequently, the method of stepwise multiple linear regression (MLR) was used to calculate the coefficients relating the descriptors to the Kováts retention index.

2.3. Artificial neural network generation

A detailed description of the theory behind a

neural network has been adequately described elsewhere [30–32]. In addition we have reported some relevant principles of ANNs in our previous papers [16,23–25]. The program for the feed-forward neural network that was trained by back-propagation strategy was written in FORTRAN 77 in our laboratory. All of the calculations presented in this work were carried out on a Hewlett-Packard 133 MHz Pentium computer, model HP Vectra VL. The descriptors appearing in the MLR model were used as inputs for generation of the ANN. Therefore the number of inputs in the ANN was six and the number of nodes in the output layer was set to be one. The number of nodes in the hidden layer was optimized. The initial weights were randomly selected from a uniform distribution that ranged between -0.3 and $+0.3$. The initial biases' values were set to be one. These values were optimized during the training of the network. The value of each input was divided to its mean value to bring the values of the input variables into the dynamic range of the sigmoid transfer function in the ANN.

Before training, the network was optimized for the number of nodes in the hidden layer, learning rates and momentum. In order to evaluate the performance of the ANN, standard error of calibration (SEC) and standard error of prediction (SEP) were used [33]. Then the network was trained using the training set by back-propagation strategy for the optimization of the values of the weights and biases.

3. Results and discussion

The data set and corresponding observed and ANN predicted values of the Kováts retention indices of all molecules studied in this work are shown in Table 1. The molecules included in the data set contain the functional groups such as alcohols, esters and ethylenic groups. All these types of molecules are included in the prediction set. Therefore, although the molecules included in the prediction set are chosen randomly they adequately represent the training set.

Table 3 shows the best MLR model obtined using the stepwise procedure. It can be seen from this table that six descriptors appeared in the MLR model. Also, the mean effect of each parameter is included in this table. Among different factors affecting the retention behavior of a molecule, mass and bulkiness are very important. The descriptors of molecular mass (M_r) and molecular volume (V) represent these properties, respectively. However, these parameters correlate with each other. Therefore, we have deleted these descriptors in generation of the MLR model and added a new descriptor called molecular density (MD). This descriptor is defined as $(M_r/V)\cdot N$, where N is the Avogadro number. The appearance of the descriptor of the electron density on the most positive atom (EDPA) in the model represents the electrostatic interaction between a terpene molecule and the polar stationary phase. The structure of many terpenes included in this study are similar to each other. These structures only differ in the arrangment of one bond or one carbon atom. Therefore, appearing of the topological descriptors such as second order Kappa index (^2K) and the path one connectivity index (^1X_p) in the model is essential. These topological descriptors encode the compactness and the degree of branching of a molecule, respectively. On the other hand, among different geometric parameters included in Table 2, two descriptors of molecular shadow surface area on $x-y$ plane (S_{xy}) and standardized molecular shadow area on $x-z$

Table 3
Specification of multiple linear regression model

Descriptor	Notation	Coefficient	Mean effect
1 Electron density on the most positive atom	EDPA	−211.479 (±28.241)	−563.65
2 Second order kappa index	^2K	82.178 (±13.122)	534.13
3 Molecular shadow surface area on x–y plane	S_{xy}	−0.442 (±0.031)	−29.50
4 Standardized molecular shadow area on x–z plane	SS_{xz}	338.954 (±22.583)	241.42
5 Molecular density	MD	6992.076 (±880.421)	630.02
6 Path one connectivity index	^1X_p	119.170 (±27.714)	594.42
Constant		5427.634 (±930.483)	

plane (SS_{xz}) appeared in the model. It is obvious that the four descriptors mentioned above can adequately differentiate between the retention behavior of the terpenes with similar structures. These parameters reveal the role of important factors such as size, degree of branching and steric interactions on the retention behavior of terpenes. The mean effects of the descriptors appearing in the model indicate that except for the geometric parameters, the electronic, topological and physicochemical parameters have a significant effect on the retention behavior of the terpenes. The calculated values of the six descriptors appearing in the best model are shown in Table 4 for all molecules included in the training and the prediction sets.

Next step was the generation of the artificial neural network. Before the training of the network, the parameters of the number of nodes in hidden layer, weights and biases learning rate and the momentum were optimized. The procedure for the optimization of these parameters is reported in our previous papers [16,25]. Table 5 shows the architecture and specification of the optimized ANN. After the optimization of ANN parameters, the network was trained using the training set for the optimization of weights and biases values. For the controlling of the overfitting of the network during the training procedure, the values of the SEC and the SEP were calculated and recorded for the monitoring the extent of learning after each 500 iterations. Fig. 1 shows the learning curve obtained from these data and reveals that after 96 000 iterations the values of SEP started to increase and overfitting was began. Therefore, training of the network was stopped at this point. From the high value of iterations two points may arise. First, the architecture of the generated ANN was correctly designed and second the descriptors appearing in the MLR model have been chosen adequately.

However, the network is a 6-5-1 ANN which has 41 adjustable parameters. On the other hand the training set consists of 41 compounds. This could lead the results due to chance. In order to show that the results are not due to chance different prediction and training sets were chosen and the network was trained using these training sets. A set of 12 compounds out of 53 molecules was chosen randomly as a prediction set each time and this procedure was repeated for three times. The results obtined are included in Table 6 for three test models. As can be seen from this table, the resuls do not depend on the

Table 4
The values of the descriptors that were used in this work[a]

Number[b]	EDPA	MD	S_{xy}	SS_{xz}	^1X_p	^2K
Training set						
1	3.7518	0.9103	71.61	0.766	4.507	8.59
2	0.8023	0.8582	59.15	0.6728	4.334	4.79
3	3.7545	0.9283	68.48	0.7127	4.507	8.59
4	3.6986	0.9409	61.11	0.7139	5.751	5.91
5	0.8010	0.8747	63.15	0.8497	4.073	6.69
6	3.6953	0.9305	62.44	0.7279	5.675	5.18
7	3.6936	0.9078	79.91	0.7075	5.956	10.17
8	3.6957	0.9455	57.70	0.7426	5.405	5.19
9	3.6852	0.9111	71.50	0.7787	5.920	8.14
10	3.6953	0.9619	65.82	0.7009	4.996	5.19
11	3.6980	0.8953	88.55	0.7512	5.936	9.07
12	3.7512	0.9273	65.86	0.6707	4.507	8.59
13	3.7010	0.9090	83.72	0.6551	5.887	9.07
14	0.8006	0.8743	58.23	0.7296	3.515	5.63
15	3.6957	0.9297	61.62	0.6968	5.675	5.19
16	3.6826	0.9227	69.50	0.714	4.805	6.48
17	3.6950	0.9456	62.54	0.7261	5.329	5.19
18	0.7991	0.8930	61.29	0.7203	3.692	5.63
19	3.6966	0.9201	72.06	0.6781	4.944	8.32
20	3.6962	0.9303	64.69	0.7116	5.675	5.19
21	0.8021	0.8582	62.59	0.7005	4.429	6.69
22	0.8021	0.8738	60.10	0.6545	3.971	4.79
23	3.6944	0.9454	54.70	0.7390	4.764	4.30
24	0.7981	0.8738	60.47	0.6394	4.048	5.63
25	3.6842	0.8937	66.85	0.7222	5.589	6.48
26	0.8028	0.8568	64.89	0.7020	4.406	6.69
27	3.6980	0.9055	77.48	0.7318	5.821	8.32
28	3.6872	0.9480	55.38	0.7420	5.324	4.68
29	3.6976	0.8906	79.57	0.7196	5.653	8.34
30	3.6843	0.9761	56.32	0.6082	4.621	5.02
31	0.8033	0.8563	62.06	0.7203	4.317	4.79
32	0.8024	0.8737	59.29	0.7049	3.971	5.63
33	3.7033	0.9139	76.53	0.7152	5.504	9.24
34	0.8013	0.8739	59.78	0.6689	4.063	6.69
35	3.7039	0.8959	87.70	0.6572	6.348	10.17
36	3.7002	0.9086	84.04	0.5795	6.348	10.17
37	0.8028	0.8403	67.10	0.7666	4.773	6.69
38	0.8043	0.8410	63.72	0.7462	4.678	4.79
39	3.6902	0.9333	57.32	0.7688	5.611	4.69
40	3.6854	0.9163	74.51	0.7368	5.420	7.30
41	0.8031	0.8415	63.61	0.7376	4.700	4.79
Prediction set						
42	3.6954	0.9619	65.82	0.7018	4.996	5.20
43	0.8029	0.8555	64.98	0.7667	4.417	6.69
44	3.7055	0.8999	81.87	0.7595	5.848	9.24
45	0.8063	0.8743	62.77	0.7857	4.063	6.69
46	3.7007	0.9142	79.79	0.6291	5.353	9.24
47	3.6986	0.9205	71.28	0.7418	4.852	7.33
48	3.6835	0.9110	74.70	0.7390	5.803	7.35
49	3.6977	0.9294	66.45	0.6908	5.675	5.20
50	3.6962	0.9303	61.45	0.7570	5.675	5.20
51	0.8054	0.8441	60.99	0.7251	4.656	5.63
52	3.6967	0.9091	86.76	0.7171	5.887	9.07
53	0.8012	0.8751	62.54	0.7275	4.048	5.63

[a] The definitions of the descriptors are given in Table 3.
[b] The numbers refer to the numbers of the molecules given in Table 1.

Table 5
Architecture of the ANN and specifications

Number of nodes in the input layer	6
Number of nodes in the hidden layer	5
Number of nodes in output layer	1
Weights learning rate	0.7
Biases learning rate	0.5
Momentum	0.5
Transfer function	Sigmodal

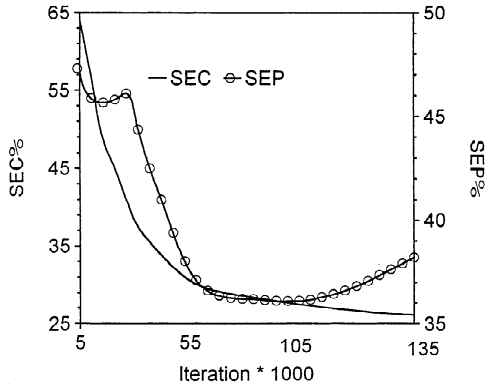

Fig. 1. A typical learning curve.

molecules of the prediction set and therefore, are not due to chance.

For the evaluation of the prediction power of the network, the trained ANN was used to predict the Kováts retention indices of the molecules included in the prediction set. Table 1 represents the experimental and predicted values of terpenes' retention indices using the generated ANN for the training and the prediction sets. The statistical parameters obtained by the ANN and MLR models are shown in Table 7. It can be seen from this Table that although the parameters appearing in the MLR model are used as inputs for the ANN, the statistics of the latter show a large improvement. In the case of the ANN, the maximum relative error for I in the prediction set was -3.48% for lavandunyl acetate and the minimum value was $+0.05\%$ for nerylisobutyrate. The mean of the relative errors between the calculated and the experimental values of the Kováts retention indices for the prediction set was 1.88%. However, it worth noting that the relative error in the experimental determination of I is in the same range.

Table 6
Comparison of the SEC and SEP of the selected model with the test models obtained using different molecules

Model	SEC (%)	SEP (%)
Selected model	28.50	38.34
Test model I	26.75	38.04
Test model II	28.11	37.11
Test model III	28.66	43.20

Table 7
Statistical parameters obtained using the ANN and MLR models[a]

Model	SEC (%)	SEP (%)	R_t	R_p	F_t	F_p
ANN	28.50	38.34	0.97	0.94	664	68
MLR	62.98	74.98	0.88	0.71	20	10

[a] t refers to the training set; p, the prediction set; R the correlation coefficient; and F is the statistical F-value.

Fig. 2 shows the plot of the ANN calculated versus the experimental I values of the prediction set. The correlation coefficient of 0.94 for this plot confirms the ability of the ANN model in prediction I for noncyclic and monocyclic terpenes. The residuals of the ANN calculated I values are plotted against the experimental values in Fig. 3. The propagation of the residuals in both sides of zero indicates that no systematic error exists in the development of the ANN.

The results of this study demonstrate that the QSPR method using the ANN techniques can generate a suitable model for the prediction of the I values of the terpenes. The descriptors appearing in the MLR model and included in the ANN give in-

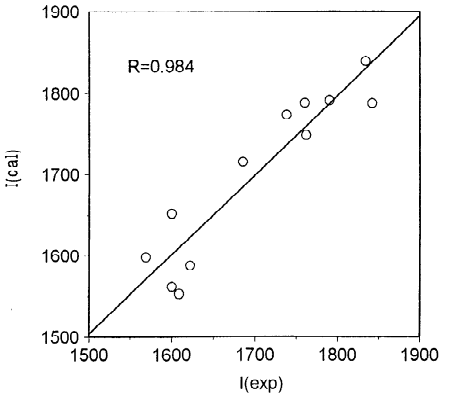

Fig. 2. Plot of the calculated retention indices against the experimental values.

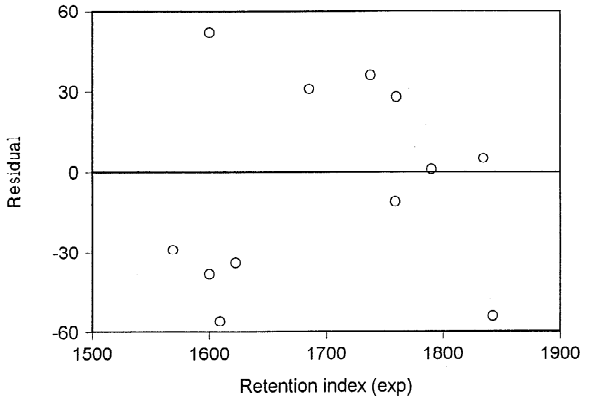

Fig. 3. Plot of the residuals vs. experimental retention indices.

formation related to the different molecular properties which can participate in the physiochemical process that occurs in GC.

References

[1] W. Jennings, T. Shibamoto, Quantitative Analysis of Flavor and Fragrance Volatile by Glass Capillary Column Gas Chromatography, Academic Press, New York, 1980.
[2] L.S. Anker, P.C. Jurs, P.A. Edwards, Anal. Chem. 62 (1990) 2676.
[3] R. Kaliszman, Structure and Retention in Chromatography, Harwood, Amsterdam, 1997.
[4] O. Mekenyan, N. Dimov, V. Enchev, Anal. Chim. Acta 260 (1992) 69.
[5] N. Dimov, A. Osman, Anal. Chim. Acta 323 (1996) 15.
[6] E.R. Collantes, W. Tong, W.J. Welsh, W.L. Zielinski, Anal. Chem. 68 (1996) 2038.
[7] A.R. Katritzky, K. Chen, V. Maran, D.A. Calson, Anal. Chem. 72 (2000) 101.
[8] T.F. Woloszyn, P.C. Jurs, Anal. Chem. 64 (1992) 3059.
[9] J. Kang, C. Cao, Z. Li, J. Chromatogr. A 799 (1998) 361.
[10] P. Payares, D. Diaz, J. Olivero, R. Vivas, I. Gomez, J. Chromatogr. A 771 (1997) 213.
[11] J.M. Sutter, T.A. Peterson, P.C. Jurs, Anal. Chim. Acta 342 (1997) 113.
[12] M. Jalali-Heravi, Z. Garakani-Nejad, J. Chromatogr. 648 (1993) 389.
[13] M. Pompe, M. Novic, J. Chem. Inf. Comput. Sci. 39 (1999) 59.
[14] A.R. Katritzky, E.S. Ignatchenko, A.R. Barcock, V.S. Lobanov, M. Karelson, Anal. Chem. 66 (1994) 1799.
[15] A.R. Katritzky, V. Lobanov, M. Karelson, R. Murugan, P.M. Grendze, J.E. Toomey, Rev. Roum. Chim. 41 (1996) 851.
[16] M. Jalali-Heravi, M.H. Fatemi, Anal. Chim. Acta 415 (2000) 95.
[17] S.L. Anker, P.C. Jurs, Anal. Chem. 64 (1992) 1157.
[18] E. Marengo, M.C. Gennaro, S. Angelino, J. Chromatogr. A 799 (1998) 47.
[19] G. Sacchero, M.C. Bruzzoniti, C. Sarzamini, E. Mentasti, H.J. Metting, P.M.J. Coenegracht, J. Chromatogr. A 799 (1998) 35.
[20] S. Agatonovic Kustrin, M. Zecevic, L.J. Zivanivic, L.G. Tucker, Anal. Chim. Acta 364 (1998) 265.
[21] K.L. Peterson, Anal. Chem. 64 (1992) 379.
[22] W.-L. Xing, X.-W. He, Anal. Chim. Acta 349 (1997) 283.
[23] M. Jalali-Heravi, F. Parastar, J. Chem. Inf. Comput. Sci. 40 (2000) 147.
[24] M. Jalali-Heravi, M.H. Fatemi, J. Chromatogr. A 825 (1998) 161.
[25] M. Jalali-Heravi, M.H. Fatemi, J. Chromatogr. A 897 (2000) 227.
[26] N.W. Davies, J. Chromatogr. 503 (1990) 1.
[27] E.K. Whalden, P.C. Jurs, Anal. Chem. 53 (1981) 484.
[28] T.R. Stouch, P.C. Jurs, J. Chem. Inf. Comput. Sci. 26 (1986) 26.
[29] J.J.P. Stewart, MOPAC, Semiempirical Molecular Orbital Program, QCPE, 455, 1983; Version 6, 1990.
[30] S. Haykin, Neural Network, Prentice Hall, Englewood Cliffs, NJ, 1994.
[31] M.T. Hagan, H.B. Demuth, M. Beal, Neural Network Design, PWS, Boston, MA, 1996.
[32] N.K. Bose, P. Liang, Neural Network Fundamentals, McGraw-Hill, New York, 1996.
[33] T.B. Blank, S.T. Brown, Anal. Chem. 65 (1993) 3084.